Electronic Supplementary Material (ESI) for Catalysis Science & Technology.

Supporting Information

Surface-Alkalinized Ti_3C_2 MXene as an Efficient Cocatalyst for Enhanced Photocatalytic CO_2 Reduction over ZnO

Junyue Li,[a,b] Ziyi Wang,[a,b] Huayu Chen,[a,b] Qiqi Zhang,[a,b] Huilin Hu,[a,b] Lequan Liu,[a,b] Jinhua Ye [a,b,c] and Defa Wang *,[a,b]

[a] TJU–NIMS International Collaboration Laboratory, Key Laboratory of Advanced Ceramics and Machining Technology (Ministry of Education, China), Tianjin Key Laboratory of Composite and Functional Materials, School of Materials Science and Engineering, Tianjin University, Tianjin 30072, China

[b] Collaborative Innovation Center of Chemical Science and Engineering, 92 Weijin Road, Tianjin 300072, China

[c] International Center of Materials Nanoarchitectonics (WPI-MANA), National Institute for Materials Science (NIMS), 1-1 Namiki, Tsukuba, Ibaraki 305-0044, Japan

---

* Corresponding author. E-mail: defawang@tju.edu.cn.

S1: Sample synthesis

The photo-deposition of platinum nanoparticles (7.5 wt%) onto ZnO was prepared by using H_2PtCl_6 as metal precursor for platinum with continuous stirring in an aqueous solution (H_2O and methanol) under a 300W Xe lamp irradiation for 1h. Then the obtained suspension was centrifuged and washed by DI water for several times. After drying in a vacuum overnight, the powders (labeled as Pt/ZnO) were obtained.

S2: Characterization

Zeta potential was tested by a zeta sizer (Zeta sizer nano ZS90, Malvern, UK) using water as a dispersant agent at 25 °C. Fourier transform infrared (FT−IR) spectra was taken from Nicolet 6700 (Thermo Scientific, USA). Brunauer−Emmett−Teller (BET) specific surface areas were measured by a nitrogen adsorption/desorption apparatus (Quantachrome Autosorb iQ2, USA). UV−Vis spectrophotometer (UV-2700, Shimadzu, Japan) was applied to obtain the UV−Vis diffuse reflection spectra. The electron spin resonance (ESR) was performed on an ESR spectrometer (JES-FA 200, JEOL, Japan) under the following conditions: scanning frequency: 9.2 GHz; central field: 328 mT; scanning width: 7.5 mT; scanning power: 2.0 mW; scanning temperature: 25 °C. The in-situ ESR experiments were carried out under a 300 W Xe lamp irradiation using 5,5-dimethyl-1-pyrroline N-oxide (DMPO) as the spin-trapped reagent to detect the signal of •OH and $O_2^{\bullet-}$. The liquid products of photocatalytic reaction were detected on a nuclear magnetic resonance (NMR) spectrometer (Avance III 400 MHz, Bruker, Germany) at 1H of magnetic field. 400 μL of DI water after reaction was collected and mixed with 100 μL of D_2O and DMSO after dilution (100 ppm) as the internal stand.

S3: Quantum yield calculation

The quantum yield (QY) was measured by using the 300 W Xe lamp with a monochromatic light filter (380 nm), and other conditions were same as in the photocatalytic activity measurements. Converting CO_2 to CO and CH_4 needs two and eight electrons, respectively. The QY was estimated by the following equations (1) and (2).[1]

$$\text{QY (CO)} = \frac{\text{two electrons for CO production} \times \text{the yield of CO}}{\text{total number of incident photons}} \times 100\% \quad (1)$$

$$\text{QY (CH4)} = \frac{\text{eight electrons for CH4 production} \times \text{the yield of CH4}}{\text{total number of incident photons}} \times 100\% \quad (2)$$

A spectroradiometer (AvaSolar-1, Avantes, America) was used to measure the number of incident photons (78.6 μmol s^{-1} m^{-2}) and average irradiation intensity (2.84 mW cm^{-2}). The yields of CO and CH_4 were 0.36 μmol and 0.13 μmol in the first hour of photocatalytic CO_2 reaction, respectively. The irradiation area of the photocatalyst was 8.04 cm^2. Total number of incident photons = 78.6 μmol s^{-1} m^{-2}×8.04 cm^2×3600 s =227.5 μmol. Based on above equations (1) and (2), the QY of CO and CH_4 over TC–OH/ZnO can be calculated as 0.32% and 0.46%.

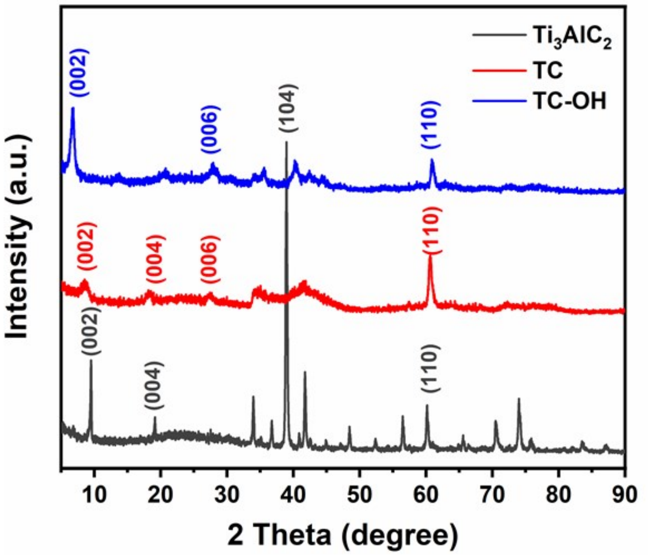

Fig. S1 XRD patterns of Ti_3AlC_2, TC and TC–OH. The characteristic diffraction peaks of as-obtained TC widened, indicating that the layer spacing of 2D TC became larger after Ti_3AlC_2 exfoliated by HF. The XRD pattern of TC–OH showed that the main characteristic diffraction peaks of TC–OH were in accordance with that of TC.

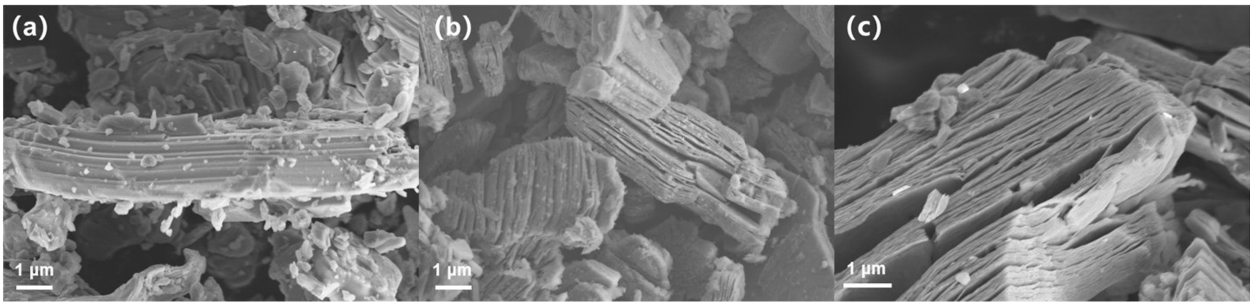

Fig. S2 SEM images of (a) Ti_3AlC_2, (b) TC, (c) TC–OH. The stacked 2D TC units were loose due to the HF etching, and the layer spacing of TC–OH expanded after surface alkalization treatment.

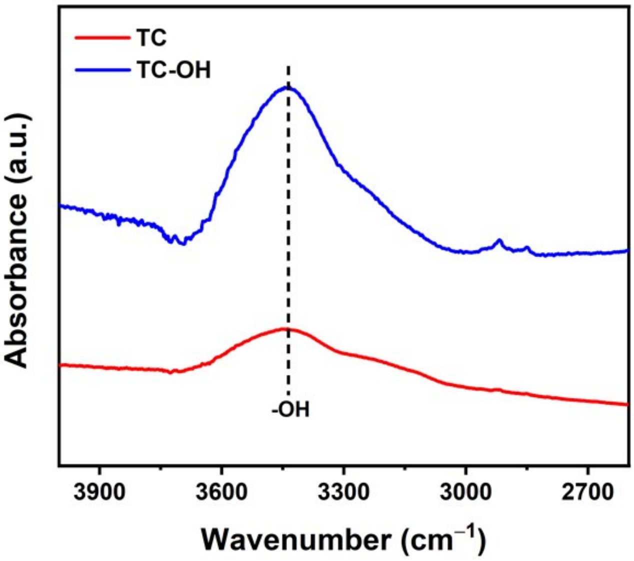

Fig. S3 FTIR spectra of TC and TC–OH. The peak (–OH stretching vibration between 3400 cm^{-1} to 3500 cm^{-1}) indicated the –F terminal groups of TC were replaced by –OH groups.

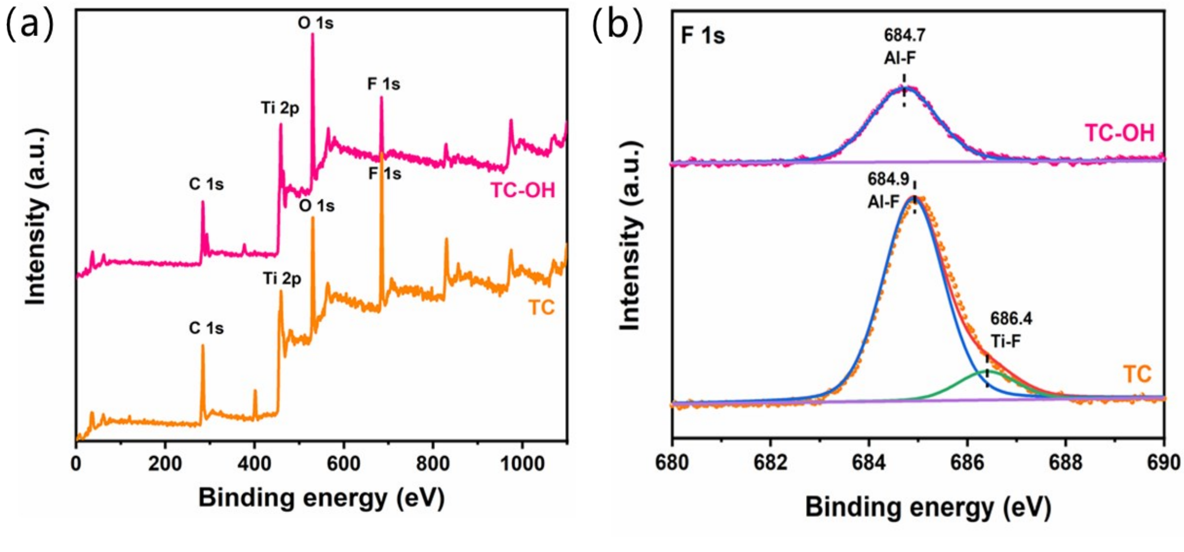

Fig. S4 (a) XPS survey of TC and TC–OH, the F1s peak decreased while the O1s peak increased after the surface alkalinization treatment. (b) High resolution XPS spectra of F 1s in TC and TC–OH.

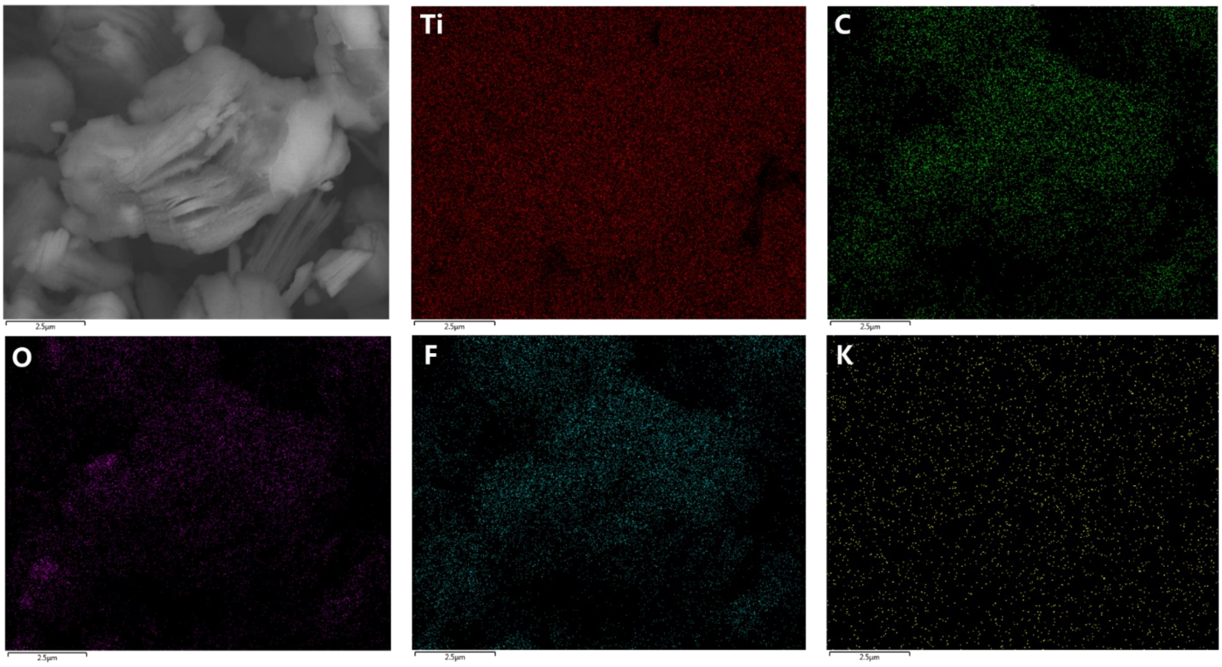

Fig. S5 SEM-EDX elemental mapping analysis of TC.

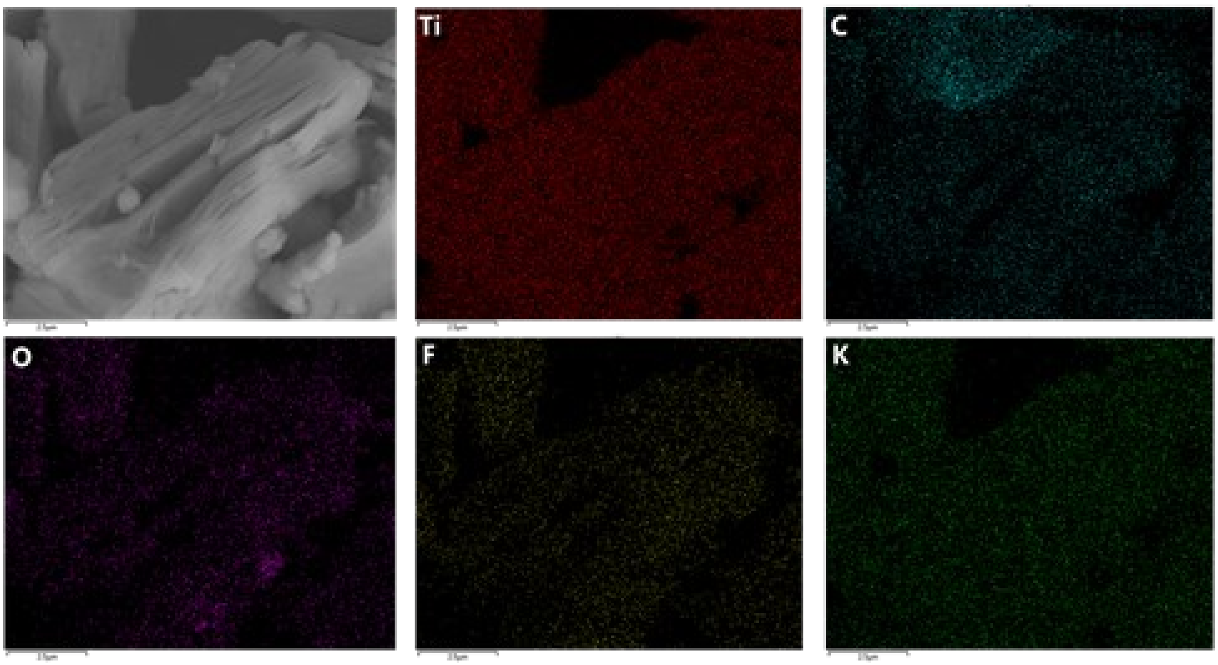

Fig. S6 SEM-EDX elemental mapping analysis of TC–OH. The F signal decreased while O and K signal increased after TC was treated by KOH, indicating the replacement of –F by –OH functional groups.

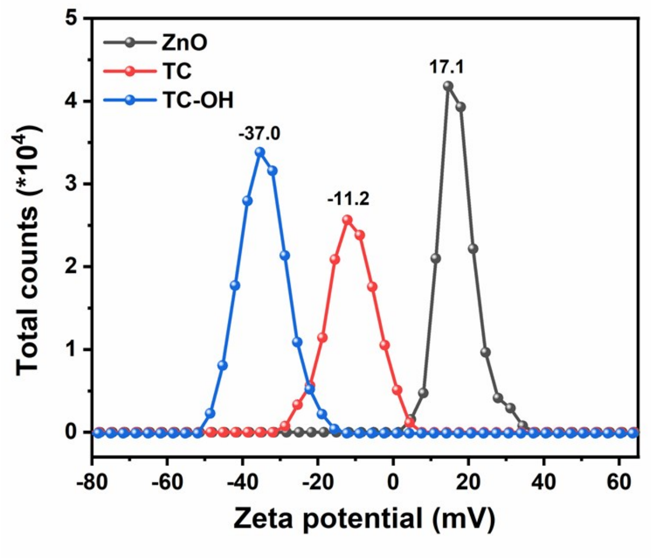

Fig. S7 Zeta potential of ZnO, TC and TC−OH (pH = 7).

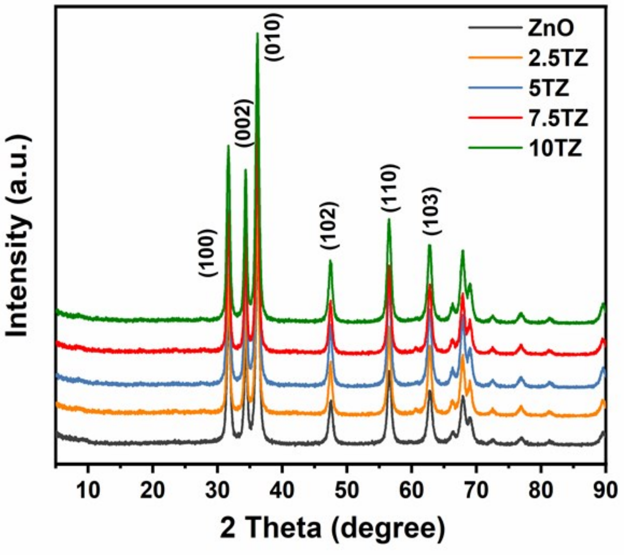

Fig. S8 XRD patterns of ZnO and XTC/ZnO (X = 2.5, 5, 7.5, 10 wt%).

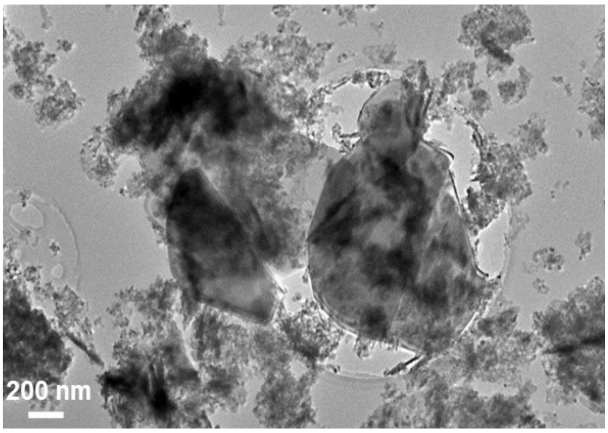

Fig. S9 TEM image of TC−OH/ZnO. The ZnO nanoparticles were mainly dispersed on the surface of TC−OH.

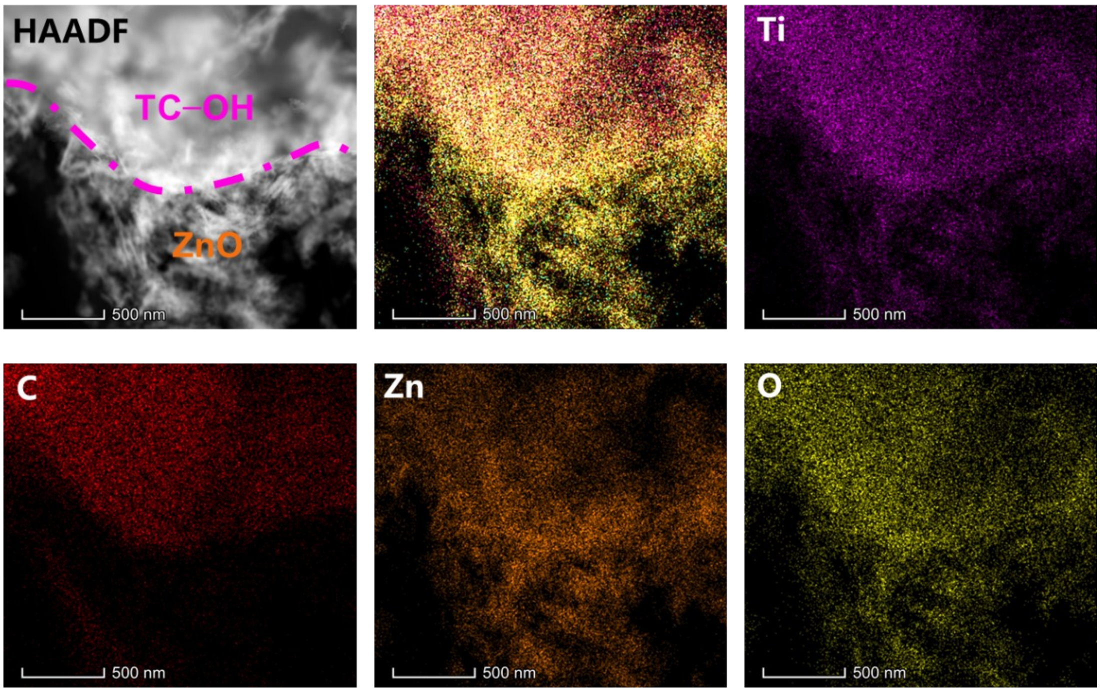

Fig. S10 TEM-EDX element mapping analysis of TC–OH/ZnO. The ZnO nanoparticles were closely anchored on the 2D stacked units of TC–OH.

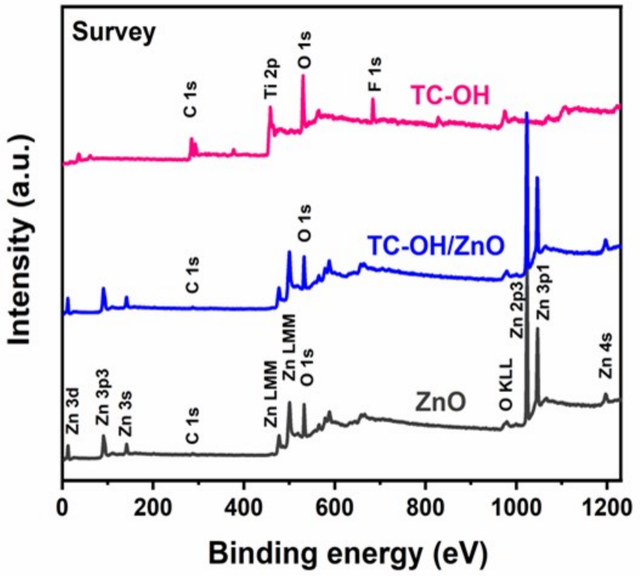

Fig. S11 XPS survey spectra of TC–OH, TC–OH/ZnO and ZnO.

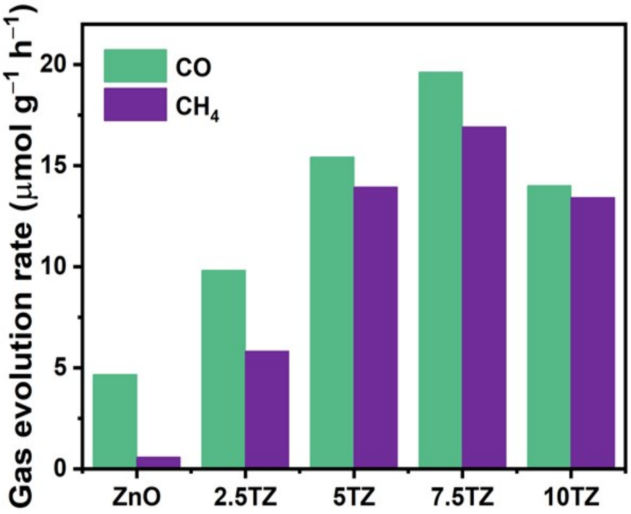

Fig. S12 Gas evolution rates of CO and CH_4 over pure ZnO and XTC/ZnO (X = 2.5, 5, 7.5, 10 wt%).

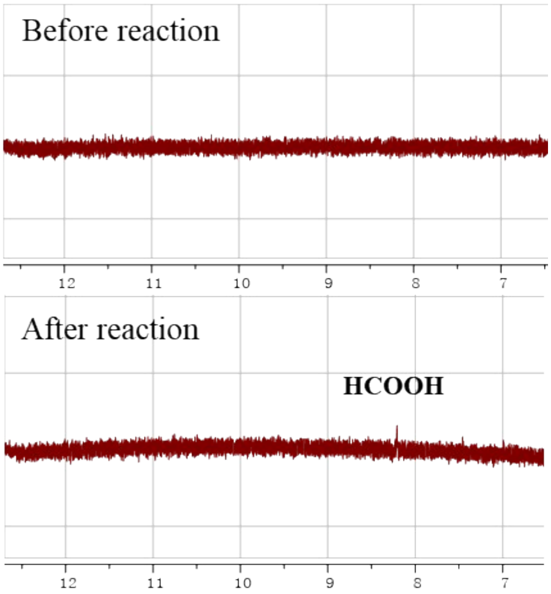

Fig. S13 NMR analysis of HCOOH in DI water over TC–OH/ZnO before and after CO_2 photoreduction reaction, showing inappreciable amount of HCOOH.

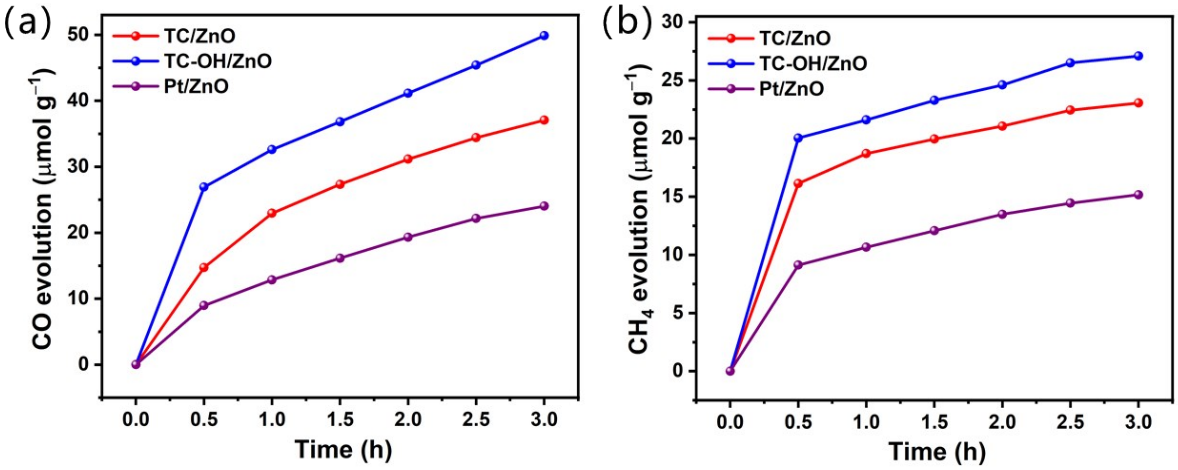

Fig. S14 (a) CO and (b) CH_4 evolution over TC/ZnO, TC–OH/ZnO and Pt/ZnO.

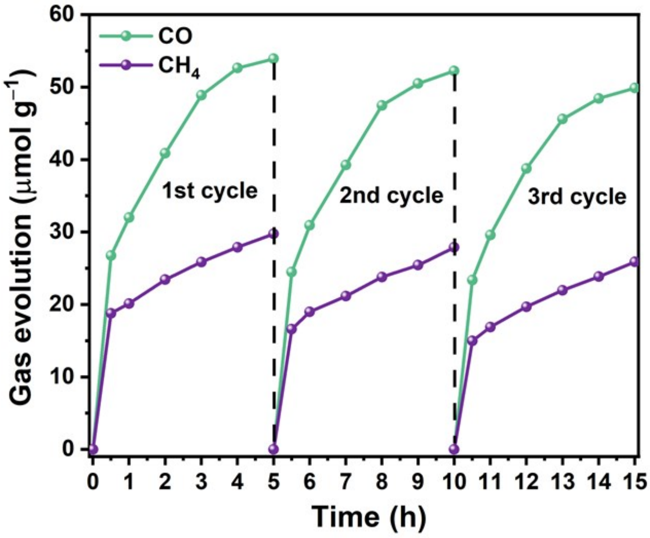

Fig. S15 Cyclic experiment of gas evolution over TC–OH/ZnO.

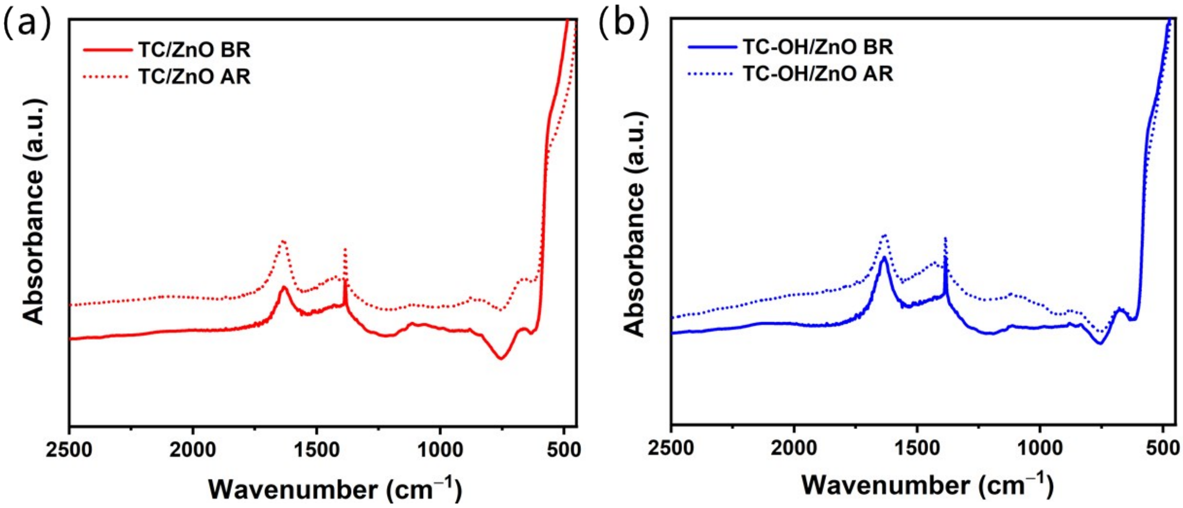

Fig. S16 FTIR spectra of (a) TC/ZnO and (b) TC–OH/ZnO before reaction (BR) and after reaction (AR) for CO_2 photoreduction.

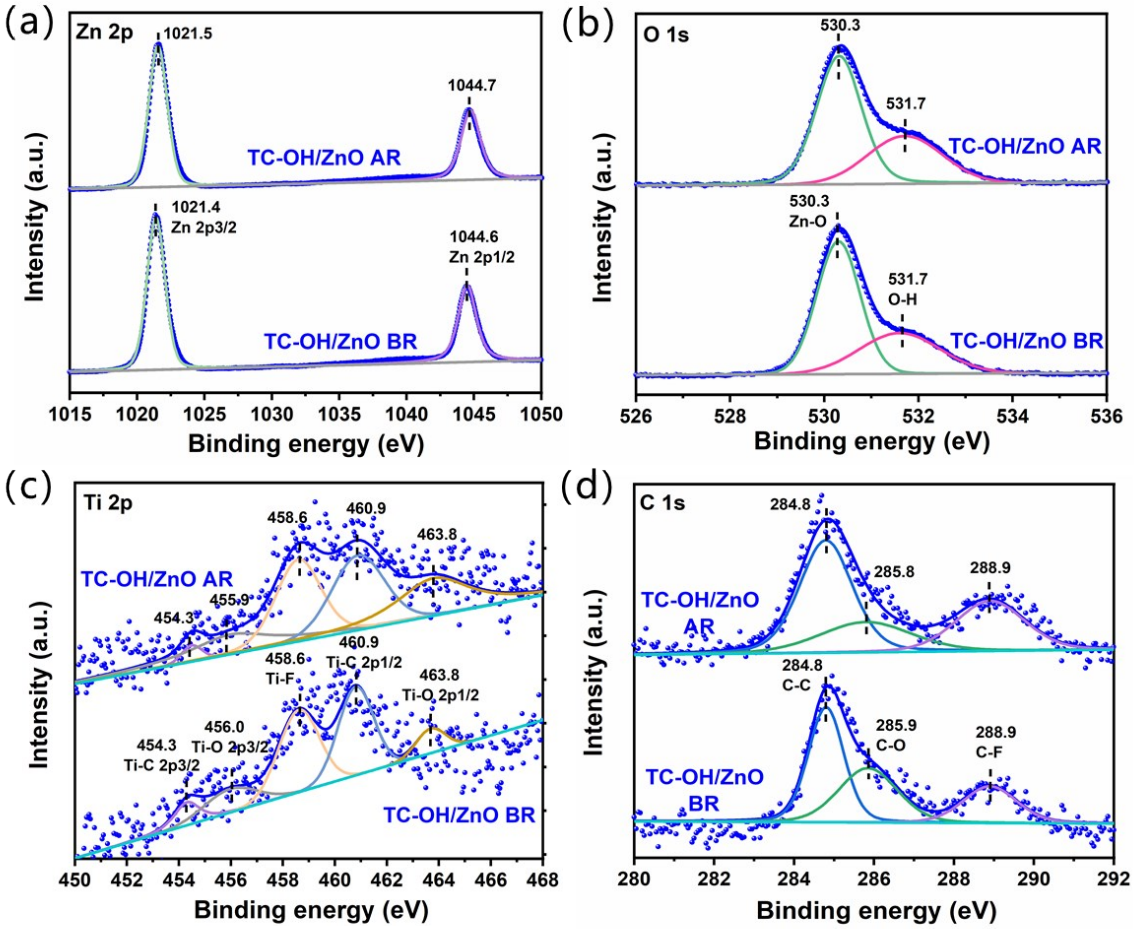

Fig. S17 High resolution XPS (a) Zn 2p, (b) O 1s, (c) Ti 2p, (d) C 1s spectra of TC−OH/ZnO before and after CO_2 photoreduction.

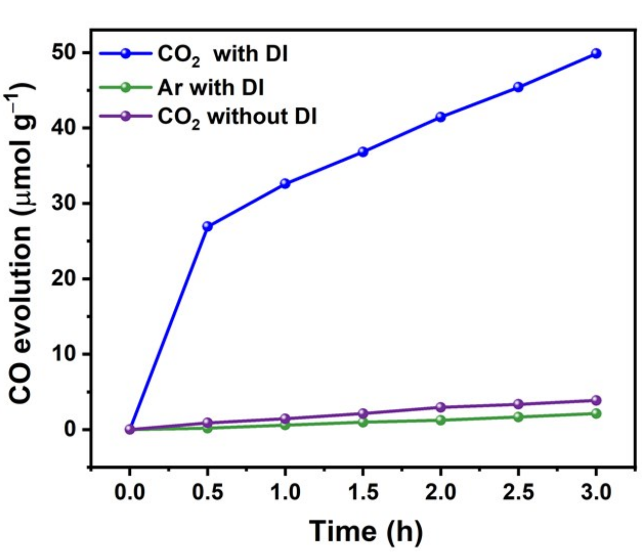

Fig. S18 Time course of CO evolution over TC−OH/ZnO under different conditions: with CO_2 gas and DI water; with Ar gas and DI water; with CO_2 gas but without DI water, the other conditions remain the same with Fig. 4a.

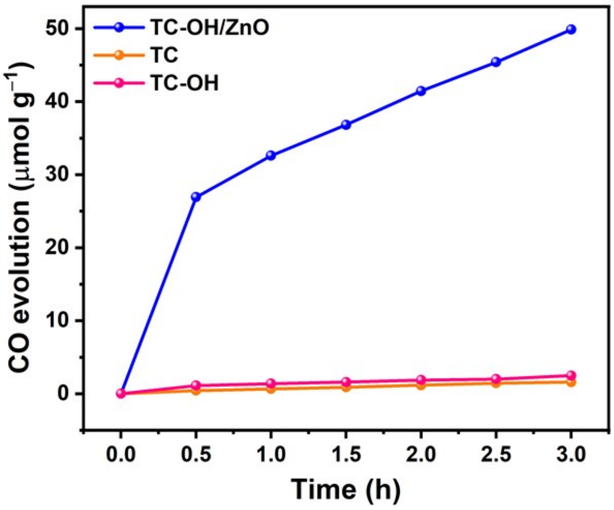

Fig. S19 Time course of CO evolution over TC−OH/ZnO, TC and TC−OH.

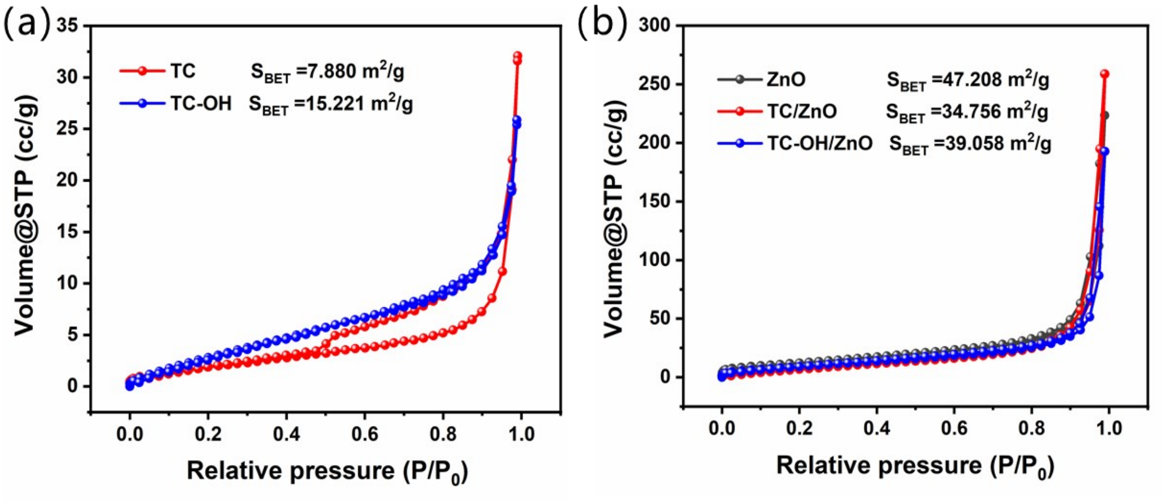

Fig. S20 BET nitrogen adsorption/desorption isotherm for (a) TC and TC−OH, (b) ZnO, TC/ZnO and TC−OH/ZnO. A larger surface area of TC−OH could expedite the combination with ZnO as well as the adsorption of CO_2 molecules. The BET surface area of ZnO was larger than TC/ZnO and TC−OH/ZnO, which could be attributed to the rather small surface area of TC and TC−OH.

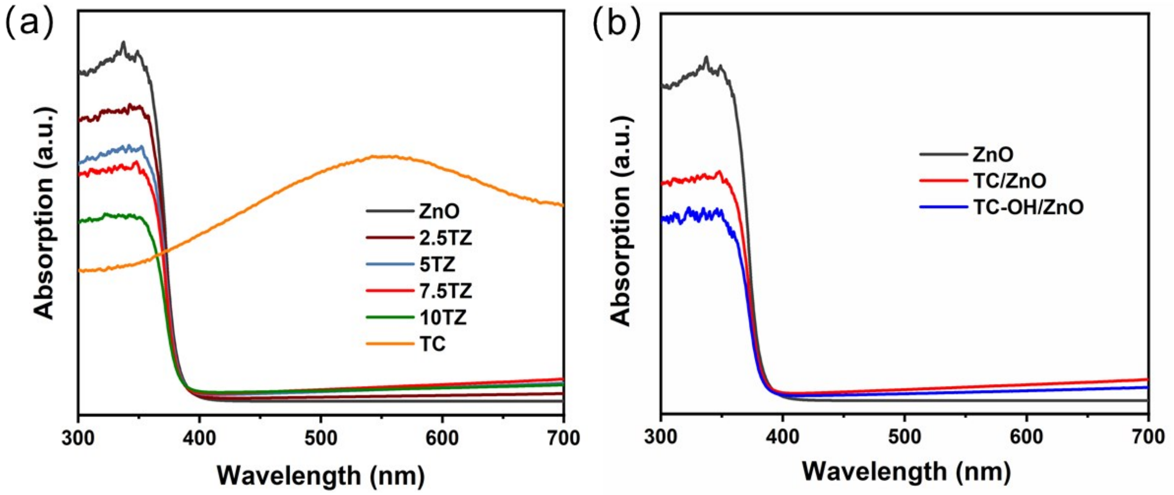

Fig. S21 UV−Vis spectra of (a) ZnO, XTC/ZnO (X = 2.5, 5, 7.5, 10 wt%) and TC; (b) ZnO, TC/ZnO and TC−OH/ZnO.

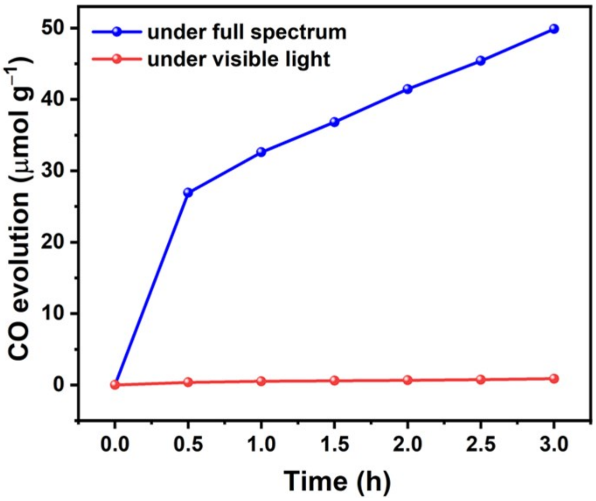

Fig. S22 Time course of CO evolution over TC−OH/ZnO under full spectrum and under visible light, using a filter to cut off the UV light, the other experimental conditions were identical to Fig. 4a.

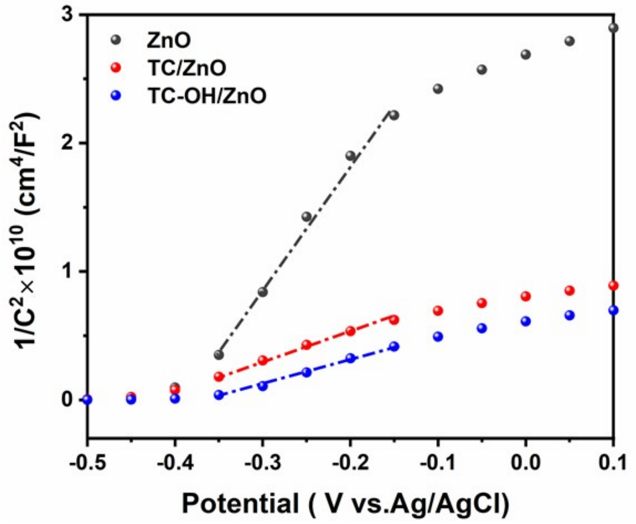

Fig. S23 Mott−Schottky curves of ZnO, TC/ZnO and TC−OH/ZnO.

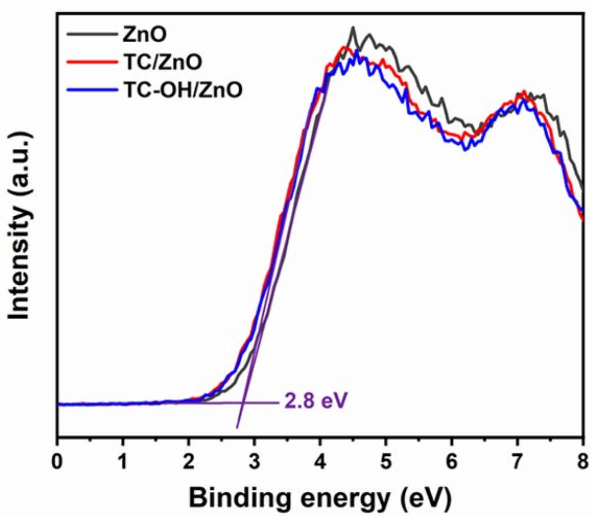

Fig. S24 Valence band XPS spectra of ZnO, TC/ZnO and TC−OH/ZnO.

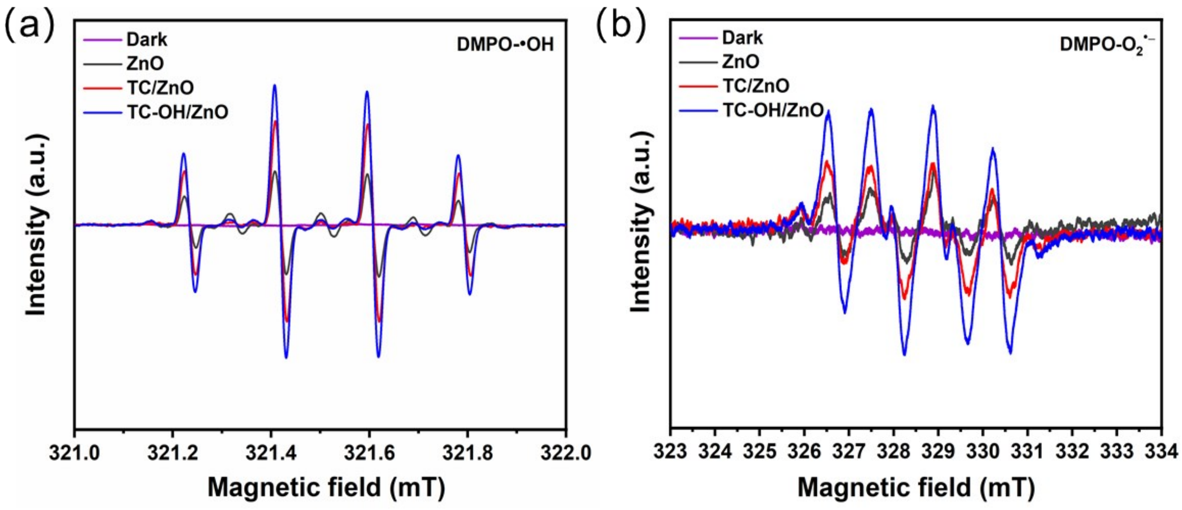

Fig. S25 ESR spectra of radical adducts signal trapped by DMPO in (a) aqueous and (b) methanol dispersions of ZnO, TC/ZnO and TC–OH/ZnO.

Table S1 The surface atomic rate of Ti, C, Al, O, F and K in the XPS spectra of TC and TC–OH.

Atomic %	Ti	C	Al	O	F	K
TC	13.04	30.74	3.72	29.01	23.49	NA
TC-OH	12.47	38.37	1.19	38.57	8.69	0.72

NA = not available

Table S2 The yields of H_2 over ZnO, TC/ZnO and TC–OH/ZnO in the photocatalytic CO_2 reduction.

Samples	ZnO	TC/ZnO	TC–OH/ZnO
Yield of H_2	0.005	0.056	0.031

Reference

1 L. L. Tan, W. J. Ong, S. P. Chai and A. R. Mohamed, *Chem. Eng. J.*, 2017, **308**, 248–255.